NASA TM-81890

3 1176 00162 8495

NASA Technical Memorandum 81890

NASA-TM-81890 19800025270

MULTI-PARAMETER YIELD ZONE MODEL FOR PREDICTING SPECTRUM CRACK GROWTH

FOR REFERENCE

NOT TO BE TAKEN FROM THIS ROOM

W. S. Johnson

SEPTEMBER 1980

LIBRARY COPY

OCT 21 1980

LANGLEY RESEARCH CENTER
LIBRARY, NASA
HAMPTON, VIRGINIA

NASA
National Aeronautics and
Space Administration

Langley Research Center
Hampton, Virginia 23665

MULTI-PARAMETER YIELD ZONE MODEL FOR PREDICTING SPECTRUM CRACK GROWTH

W. S. Johnson
NASA Langley Research Center
Hampton, Virginia 23665

ABSTRACT

A systematic technique is presented for modeling crack growth load interaction effects due to spectrum loading. The Multi-Parameter Yield Zone (MPYZ) model accounts for crack growth retardation, acceleration, and underload effects. The load interactions are attributed to the residual stress intensity due to the plastic deformation at the crack tip. As part of an ASTM E24.06.01 round-robin effort, fatigue crack growth was predicted and compared with test data for a variety of spectrum loadings.

LIST OF SYMBOLS

A	ratio of K_{max}^{OL}/K_{max} above which no retardation occurs
a	half surface crack length, m
a_{ap}	half crack length when current stress applied
a_f	final half crack length of crack growth prediction
a_i	initial half crack length of crack growth prediction
a_{OL}	half crack length when overload applied
B	ratio of K_{max}^{OL}/K_{max} for single overload below which no crack growth occurs
B'	ratio of K_{max}^{OL}/K_{max} for any number of overloads below which no crack growth occurs

N80-33778 #

b	specimen half width, m
C	material crack growth constant
K_c	critical stress intensity factor for material, $MN\text{-}m^{-3/2}$
K_{max}	currently applied maximum stress intensity, $MN\text{-}m^{-3/2}$
K_{max}^{eff}	effective applied maximum stress intensity after load interaction, $MN\text{-}m^{-3/2}$
K_{max}^{OL}	overload maximum stress intensity, $MN\text{-}m^{-3/2}$
K_{min}	currently applied minimum stress intensity, $MN\text{-}m^{-3/2}$
K_{min}^{eff}	effective applied minimum stress intensity after load interaction, $MN\text{-}m^{-3/2}$
K_{OL}	overload maximum stress intensity that is still effective prior to an underload, $MN\text{-}m^{-3/2}$
K_{pr}	the minimum stress intensity associated with the K_{max}^{OL} cycle, $MN\text{-}m^{-3/2}$
K_R	the residual stress intensity associated with the MPYZ load interaction model, $MN\text{-}m^{-3/2}$
K_R^W	the residual stress intensity associated with the Willenborg retardation model, $MN\text{-}m^{-3/2}$
K_{UL}	current underload stress intensity, $MN\text{-}m^{-3/2}$
n	material crack growth constant
R	stress ratio, S_{min}/S_{max}
R^{eff}	stress ratio after load interaction, $K_{min}^{eff}/K_{max}^{eff}$
R_L	ratio of current underload stress to maximum overload stress, S_{UL}/S_{max}^{OL}
R_{max}	stress state dependent maximum value of R^{eff}

S_{max}^{OL}	maximum overload stress, MPa
S_{pr}	minimum stress associated with overload cycle, MPa
S_{UL}	underload stress, MPa
Y	value of β below which overload is unaffected
Z	value of β above which there is no overload effect
Z_{ap}	plastic zone diameter associated with currently applied load, m
Z_{OL}	plastic zone created by overload, m
α	1 for plane stress
	3 for plane strain
β	underload factor, $\left(K_{pr} - K_{UL}\right)/\left(K_{eff}^{OL} - K_{UL}\right)$
Δa	crack growth increment since overload applied, $a_{OL} - a_{ap}$, m
ΔK	stress intensity range, $K_{max} - K_{min}$, MN-m$^{-3/2}$
ΔK_{TH}	threshold stress intensity range at $R = 0.0$, MN-m$^{-3/2}$
ΔK_{TH}^{*}	threshold stress intensity range for a given R^{eff}, MN-m$^{-3/2}$
π	constant 3.141592654
σ	remote field stress, MPa
σ_{YS}	material yield stress, MPa

INTRODUCTION

The early 1970's saw three significant concepts generated to deal with spectrum effects on crack propagation. They analytically accounted for the experimentally observed phenomenon of crack growth retardation [1-3]. These three approaches, commonly referred to as the Wheeler model, the Willenborg model, and the Elber (or crack closure) model, along with the creation of large and efficient digital computers, spurred the aircraft industry to analytically predict crack growth from realistic spectrum loadings. The Wheeler model is characterized by a shape-fitting parameter, "m", that must

be experimentally determined for each condition of material, loading, and environment that is of interest. The Willenborg model, on the other hand, does not incorporate an empirical shape factor but uses the material yield stress to give a plastic zone size, which is then used to calculate crack retardation. Although the Willenborg model does not incorporate a "fudge" factor, its predictions are not always satisfactory. The Elber model is based on the crack-closure phenomenon and uses an effective stress intensity which is based upon the stress needed to open the crack. The closure factor in the Elber model is determined experimentally from constant-amplitude data. The Elber model has been used in the aerospace community with limited success. These models have been modified by various investigators during the past five years with some degree of success [4-7].

Recent testing at General Dynamics [8-9], as well as work performed by Hillberry [10-12] and others [13-14], have shown that various loading parameters that are not included in the Wheeler or Willenborg models (such as crack growth acceleration and underloads) have a significant effect on spectrum crack growth.

This paper will present a phenomenological load interaction model referred to as the Multi-Parameter Yield Zone (MPYZ) load interaction model. It is a subprogram within the computerized crack growth program CGR in references 15 and 16. The crack growth model is discussed first, followed by the load interaction model. The load interaction model is described in three sections: retardation, acceleration, and underload effects. The crack growth predictions are discussed and compared with the experimental results. The present study was part of a round-robin effort that was sponsored by ASTM Subcommittee E24.06. The purpose of this round-robin effort was to

compare various methods for predicting crack growth through center cracks in 2219-T851 aluminum alloy center-crack tension specimens subjected to aircraft-type spectrum loadings. The data used for the round robin were generated by Chang and Stolpestad [17] under an Air Force sponsored contract. All material data in this paper can be found in reference 17, except as noted.

CRACK GROWTH MODEL

Numerous fatigue crack propagation models have been proposed in the literature to describe the relationship between the crack growth rate, da/dN, and the stress intensity range, ΔK. Many of these relationships consider such parameter as stress ratio, R, and fracture toughness, K_c. Gallagher [Gallagher, J. P., "Fatigue Crack Growth Rate Laws Accounting for Stress Ratio Effects," ASTM Task Force E24.04.04, Report No. 1, 1974.] has summarized a number of these models.

The Forman [24] crack growth model provides a good fit for the constant amplitude 2219-T851 aluminum crack growth data furnished for the spectrum crack growth prediction round-robin. For the present study, the Forman equation was slightly altered to the following form:

$$da/dN = \frac{C\,\Delta K^n}{(1 - R^{eff})^m K_c - \Delta K} \tag{1}$$

where

$m = 1$ at $R \geq 0$

$m = 2$ at $R < 0$

The equation is exactly that suggested by Forman except for the m exponent applied to the stress ratio. The exponent $m = 2.0$ for negative R^{eff} values. Equation (1) accounts for the crack growth behavior

by using the full stress intensity range, ΔK, and the corresponding R^{eff} values, i.e., the stress range includes compressive portions. Load interaction effects are accounted for by adjusting R^{eff} during each cycle, so R^{eff} does not necessarily equal the actual stress ratio of the current cycle. Most of the present paper is about the procedure used to find the proper values of R^{eff} to account for retardation, acceleration, and underload effects. The parameters C and n were found from the supplied constant amplitude crack growth data [17] by a least-squares regression analysis. The critical stress intensity factor, K_c, was chosen to be 88 $MN\text{-}m^{-3/2}$ (80 ksi $\sqrt{in.}$), which resulted in $C = 3.68 \times 10^9$ and $n = 3.232$.

The author has formulated an opinion from observed crack growth behavior, and from crack closure considerations of Newman [19], that the maximum effective stress ratio is a function of the constraint at the crack tip due to the different stress states, i.e., plane-stress or plane-strain or in between. Therefore a simple relationship has been used to determine the maximum allowable stress ratio used in equation (1):

$$R_{max} = [Z/t \times 0.2] + 0.6 \tag{2}$$

where $Z = \frac{1}{\alpha\pi}\left(\frac{K_{max}}{\sigma_y}\right)^2$ is the plastic zone diameter for the applied K_{max}, t is the material thickness, and α is 1.0 or 3.0 for plane stress or strain assumption, respectively. Notice that for plane-strain ($Z/t \rightarrow 0$) so that $R_{max} = 0.6$. Therefore if an applied cycle had a stress ratio equal to 0.75, but was cycled in a plane-strain region, a value of approximately 0.6 would be used in equation (1) for R^{eff}. If the plastic zone diameter

equals or exceeds the thickness, then a state of plane-stress is assumed, and $R_{max} = 0.8$, i.e., maximum value for R^{eff} in equation (1) is 0.8.

Figure 1 depicts the fit of equation (1) to the data. The solid line represents perfect correlation while the dashed lines represent a factor of two discrepancy. The constant amplitude data consisted of R values between -1.0 and 0.7 and maximum stress levels from 55.2 to 276 MPa. Figure 1 is a plot of the predicted crack growth rates versus the actual growth data used to evaluate the C and n in equation (1). Several constant amplitude tests at 276 MPa (40 ksi) were not included because of net section yielding; the author did not want to bias the crack growth equation for this extreme case. It is interesting to note that equation (1) does a good job of correlating the negative and positive stress ratios.

Typically, many cycles in a variable-amplitude loading program produce stress intensity ranges, ΔK's, that are so small no crack growth results. The threshold stress intensity range, ΔK^*_{TH}, is stress ratio dependent and is not accounted for in the modified Forman equation. If the applied ΔK is less than ΔK^*_{TH}, then equation (1) is not applicable and no crack growth results. The threshold for each cycle, ΔK^*_{TH}, was calculated from a read in value of ΔK_{TH} at $R = 0.0$, as defined from constant amplitude data, such that

$$\Delta K^*_{TH} = (1 - R^{eff})\Delta K_{TH} \tag{3}$$

where ΔK_{TH} is, from basic data [20], taken to be 3.3 MN-m$^{-3/2}$ for 2219-T851 aluminum alloy.

A method for assessing constant amplitude crack growth data as well as an efficient and accurate crack growth accumulation/integration routine for

the Forman equation have been previously presented by the author in reference 21 and will not be repeated herein.

In summary, then, to calculate an increment of crack growth equation (1) is used. Two situations may exist; ΔK is below threshold, and $da/dN = 0$; or ΔK is above threshold, and load interaction effects are taken into account by properly adjusting the effective stress ratio, R^{eff}. Most of the remainder of this paper describes the procedures used to determine the proper values of R^{eff} to be used in equation (1) during each load cycle.

LOAD INTERACTION MODEL

Realistic aircraft loading results in a mixture of high and low stresses associated with varying stress ranges. The influence of any given load cycle on crack growth behavior depends upon the prior load history, thus the term "load interaction" is used to describe these effects. The load interaction model used by the author to predict crack growth under spectrum loading is referred to as the Multi-Parameter Yield Zone (MPYZ) model. The MPYZ is a phenomenological model that is intended to account for such recognized load interactions as retardation caused by previous overloads, acceleration due to current overloads, and underload effects. Retardation results in less crack growth for a given load cycle than would be produced under the same constant amplitude condition. Conversely, acceleration results in more crack growth than would be expected under constant amplitude. The underloads result in a reduction of the retardation effects of the current overload.

The MPYZ model began in 1973 [15] as a form of the Willenborg retardation model [2]. During 1976, in reference 21, two parameters were added to the Willenborg model. These parameters correspond to ratios of a single

overload stress intensity to the following applied stress intensity that resulted in (1) no crack growth retardation (parameter A) or (2) complete crack growth retardation (parameter B). Parameter B is very similar to the "shut-off" ratio implemented by Gallagher [16].

In the present model, load interaction effects are calculated utilizing a residual stress intensity, K_R, concept. Crack growth retardation and acceleration are accounted for by decreasing or increasing, respectively, the effective stress ratio used in a modified Forman crack growth equation. The R^{eff} is a function of the residual stress intensity, K_R, and the currently applied stress intensity. The effective stress range that is used to calculate crack growth remains the same, but the mean of the stress range is altered by K_R to account for the appropriate load interaction. The stress ratio corresponding to a load interaction will be designated R^{eff} and defined as follows:

$$R^{eff} = \frac{K_{min} - K_R}{K_{max} - K_R} = \frac{K^{eff}_{min}}{K^{eff}_{max}} \tag{4}$$

where K_R is the residual stress intensity which will be discussed in the following section. The K_R will be positive or negative depending on whether the load interaction produces retardation or acceleration, respectively. The maximum allowable value of R^{eff} is R_{max} as defined in equation (2). A simplified flow chart of the MPYZ model in the CGR computer program is presented in figure 2. The three primary phenomenological events of load interaction, i.e., retardation, acceleration, and underload effects, will be addressed in the following sections.

Retardation

The amount of crack growth retardation for a given applied cycle depends upon the applied loading as well as the extent of crack growth into the overload plastic zone, as suggested by Willenborg, Engle, and Wood [2]. Gallagher [5] expressed the Willenborg model as

$$K_R^W = K_{max}^{OL}\left(1 - \frac{\Delta a}{Z_{OL}}\right)^{1/2} - K_{max} \tag{5}$$

where K_R^W is the Willenborg residual stress intensity factor; K_{max}^{OL} is the maximum stress intensity for the overload cycle; K_{max} is the maximum stress intensity for the current load cycle; Δa is the crack growth increment between the overload cycle and the current cycle as depicted in figure 3. The Willenborg model applies Z_{OL} as the plastic zone <u>radius</u> associated with K_{max}^{OL}. But in the present MPYZ model, Z_{OL} is defined as the zone <u>diameter</u> such that

$$Z_{OL} = \frac{1}{\alpha\pi}\left(\frac{K_{max}^{OL}}{\sigma_{YS}}\right)^2 \tag{6}$$

where

α = plastic zone constraint factor

= 3, plane strain

= 1, plane strain

σ_{YS} = material yield stress

The plastic zone diameter is used to calculate K_R^W. Mills, Hertzberg, and Roberts [18] have shown that the retardation effects last approximately one plastic zone diameter in A514F steel. Himmelein and Hillberry [11] present

data that also imply the overload is effective over the plastic zone diameter for 2024-T6 aluminum.

The residual stress intensity, K_R^W, calculated in equation (5) physically represents the difference between the stress intensity required to produce a current plastic zone equal to $Z_{OL} - \Delta a$ and the current applied stress intensity, K_{max}. Retardation occurs when K_R^W is greater than zero. In such cases the residual stress intensity at the crack tip is greater than that for an equivalent constant amplitude case, so there is less crack growth, i.e., retardation.

Figure 4 presents a typical aircraft load sequence. Notice that the overload and underload are labeled. The dashed line represents the decay in effective overload stress intensity, K_{OL}^{eff}. The value of K_{OL}^{eff} decreases with each cycle of crack growth.

Gallagher and Hughes [5] introduced a proportionality factor, ϕ_R, such that

$$K_R = \phi_R K_R^W \tag{7}$$

The ϕ_R term adjusts the amount of retardation according to several material and load history parameters. Notice that the higher the value of ϕ_R the more the retardation.

The MPYZ load interaction model incorporates

$$\phi_R = \left[1.0 - (K_{TH}/K_{max})\right] \Big/ \left[(\psi - 1.0) \times (1.0 - R_L)\right] \tag{8}$$

where

$\psi = B/A$; A = the ratio of K_{max}^{OL} to K_{max} below which no retardation takes place (no-retardation ratio)

B = the ratio of K_{max}^{OL} to K_{max} above which no crack growth is produced (shut-off overload ratio)

$R_L = S_{UL}/S_{max}^{OL}$; ratio of current underload stress to current overload stress.

The $\left[1.0 - (K_{TH}/K_{max})\right]$ factor accounts for the threshold level of crack growth. The $(\psi - 1.0)$ factor adjusts the retardation between the shut-off overload ratio B and the no-retardation ratio A as shown in figure 5. The $(1.0 - R_L)$ expression adjusts the amount of retardation according to the cyclic range of the spectrum. Similar spectra that differ only in the minimum underload will have different overall retardation. This phenomenon is also observed in crack closure [19] where the maximum and minimum stresses in a spectrum usually set the crack opening stresses therefore controlling retardation. Notice that a spectrum with negative minimum (i.e., negative value of R_L) will produce less retardation for a given ratio of K_{max}^{OL}/K_{max} than a similar loading sequence with a positive minimum stress.

Parameters A and B are considered to be material dependent parameters. Ideally, A and B can be determined for a given material by conducting a series of well controlled systematic single overload tests. The ratio of the applied single overload stress to the following stress is varied from test to test in order to ascertain the limiting ratios that (1) produce no overload effect (i.e., ratio = A) and (2) produce no crack growth other than that produced by the overload (i.e., ratio = B). The types of tests conducted by Probst and Hillberry [12] are suited to this purpose. If these

systematic test results are not available for evaluation for a particular material, one has to try various combinations of A and B to predict crack growth and compare the predictions with available test results. Typical values of A and B found in the literature range from 1.0 to 1.5 and 1.8 to 2.5, respectively, for various materials.

The MPYZ load interaction model uses a simple algorithm to account for multiple overload effects [13]. Simply stated, the more overload cycles one has in succession the greater the retardation effect, i.e., the lower the value of B'. Thus this relationship is approximated for 2219-T851 aluminum by

$$B' = \left(\frac{B - 2.0}{N_{OL}}\right) + 2.0 \tag{9}$$

where

B' = the value of B to be used in equation (8)

N_{OL} = the number of overloads applied in succession

The 2.0 is considered to be a lower bound for B' after many overloads for 2219 aluminum alloy

Although the equation is simple, it accounted for the multiple overload effects in reference 17 quite well.

Acceleration

The crack growth during an overload cycle has been observed to be larger than one might expect from constant amplitude data [14]. This phenomenon is referred to as crack growth acceleration. The acceleration may be attributed to the crack and the resulting crack tip plastic zone growing into an area with less residual stress intensity than that of an equivalent constant

amplitude case, so that crack growth is less inhibited. For example, imagine that the plastic zone diameter, Z_{ap}, in figure 2 was caused by a large enough load such that

$$\Delta a + Z_{ap} > Z_{OL} \tag{10}$$

This would result in a crack growth acceleration for the applied cycle.

Equation (4) is also utilized for acceleration load interaction. When inequality (10) is true, acceleration occurs, and K_R^W is a negative value.

The MPYZ load interaction model incorporates an acceleration adjustment term, ϕ_A, for K_R^W defined as

$$\phi_A = (1.0 - R_L) \tag{11}$$

where the term $(1.0 - R_L)$ adjusts the amount of acceleration depending on the ratio of the current underload stress to the overload stress. Thus the residual stress intensity used in equation (4) is defined as

$$K_R = \phi_A K_R^W \tag{12}$$

for acceleration. Note that ϕ_A is used to calculate K_R when K_R^W is a negative value. Thus, the effective stress ratio, R^{eff}, will increase.

Underload Effects

Occasionally in spectrum aircraft-type loading, a rather significant compressive load or a tensile load occurs that is lower than most of the previous minimum loads. This load, S_{UL}, is defined as an "underload," as depicted in figure 4. An underload has dramatic influence because it can significantly reduce retardation. The author has conducted tests to establish

the effect on crack growth caused by deleting the compressive stresses from a fighter cycle-by-cycle spectrum. These tests were conducted on 7475-T7651 aluminum in Sump Tank Water (STW) at a maximum spectrum stress of 214 MPa (31 ksi). The fighter spectrum contains relatively few compressive loads for the wing root bending moment spectrum. Those that are present have magnitudes less than 15 percent of the maximum tensile load. As shown in figure 6, the deletion of these few small compressive stresses resulted in a 50 percent increase in life. This substantial increase in crack growth rate cannot be attributed solely to the compressive load excursion increasing the stress range and producing a negative stress ratio. Rather, the negative stresses tend to negate the crack growth retardation caused by previous tensile overloads.

Hillberry and associates [10-12] have conducted several studies into this particular phenomenon. In reference 10 underloads of varying amplitude were applied immediately after an overload to assess the effect of each underload amplitude on the following crack propagation behavior. These data are very useful in modeling the underload phenomenon. Chang and Stolpestad [17] also have conducted several simple variable amplitude tests that lend themselves to characterizing the effects of underloads.

In actual aircraft load histories, a significant underload may not immediately follow a large overload. Therefore, in order to generalize the model to realistic spectrum loadings, an effective overload is computed whenever an underload cycle is applied. The effective overload represents the remaining contribution of K_{max}^{OL} before underload application, to simulate the conditions of Hillsberry's data upon which the following model is based.

The effective overload is assumed to be the load required to create a plastic zone size of $Z_{OL} - \Delta a$ in figure 3. The effective overload stress intensity is therefore equal to K_{eff}^{OL} where

$$K_{eff}^{OL} = K_{max}^{OL} \left(1 - \frac{\Delta a}{Z_{OL}}\right)^{1/2} \tag{13}$$

The underload is accounted for by reducing the effective overload stress intensity factor using the ratio

$$\beta = \frac{K_{pr} - K_{UL}}{K_{eff}^{OL} - K_{UL}} \tag{14}$$

where K_{pr}, K_{eff}^{OL}, and K_{UL} are shown in figure 4. K_{pr} is the minimum value of stress intensity before the overload. Thus a new effective overload stress intensity factor, denoted K_{OL}', is computed and used in accounting for crack growth retardation. The value of this effective overload stress intensity, K_{OL}', is expressed as

$$K_{OL}' = \frac{K_{eff}^{OL}}{Z - Y} (Z - \beta) + K_{max} \tag{15}$$

where Z is the value of β above which K_{OL}' is K_{max} and Y is the value of β below which $K_{OL}' = K_{eff}^{OL}$. Thus, Y determines when the underload does not reduce the amount of retardation, and Z determines when no retardation occurs. The relationship among these variables is indicated in figure 7.

Notice, in figure 7, that when $\beta < Y$ the underload has no effect on retardation and K_{OL}' equals K_{eff}^{OL}. Likewise, when β is greater

than Z, K'_{OL} equals K_{max} so no retardation results. If β is between the values of Y and Z the effective overload, K^{eff}_{OL}, is reduced. The relationship between β and K'_{OL} depends on the values of Y and Z and can be represented by a straight line.

The Y and Z for the particular material must be determined in a similar fashion as that for A and B. Carefully controlled crack growth tests can be run in a systematic manner to completely determine the crack growth load interaction behavior. Tests as conducted in reference 10 are ideal for the determination of Y and Z.

RESULTS OF SPECTRUM CRACK GROWTH PREDICTIONS

The crack growth prediction computer program, CGR-LaRC (an updated version of CGR [15,16]), was used to make predictions for the present round-robin tests. The program required the usual descriptions of shape and material properties of the test specimen to be analyzed. In addition the program required the four load interaction parameters A, B, Y, and Z as discussed in the previous section. These parameters, as well as the material data for the 2219-T851 aluminum, are presented in table 1. Notice that A = 1.0 and Y = 0.0 such that there are essentially only two load interaction parameters used to describe 2219-T851 aluminum, B and Z. The B = 2.3 agrees with data presented in reference 12.

Reference 17 contained many simple single overload tests. The tests were not systematic (i.e., each test conducted at an incrementally different value of overload ratio) but they did cover a wide range of overload ratios, $\frac{K^{OL}_{max}}{K_{max}}$. The A, B, Y, and Z terms were selected from the simple overload

test observations and to provide the best fit of the predicted to the experimental test results for these simple tests.

The round-robin program consisted of 13 tests. Five basic aircraft type spectra were used. Three of the spectra were applied at three different load factors (i.e., different scaling of the stresses) and two spectra were applied at two different load factors. There was only one test per individual spectrum. More details are available in reference 17.

The round-robin specimens contained a through center crack. The secant correction factor was used to calculate the stress intensity factor [23]:

$$K = \sigma \sqrt{\pi a} \qquad \sqrt{\sec \frac{\pi a}{2b}} \tag{16}$$

where

σ = the remote stress

a = half surface crack length

b = half specimen width.

Figure 8 is a plot of the predicted lives versus the test lives from the 13 tests in the round-robin effort. The solid line represents exact predictions. The dashed lines are a factor of two high or low. The mean and standard deviations of the ratio of predicted life to test life are 0.97 and 0.24, respectively. The standard error for the 13 test predictions is

$$\text{S.E.} = \frac{\sum \left| 1 - \frac{N_{pred}}{N_{test}} \right|}{13} = 0.18$$

Figure 9 presents the predicted and experimental crack growth curves of specimens M-90, M-91, and M-92 for comparison. The shape of the predicted crack growth curve is in excellent agreement with that of the experimental.

All of the predictions were within a factor of 1.5 of the test results. In general, all predictions were extremely good with M-88 and M-89 being the poorest. (See table 2.) Notice in this table that the ratio of the predicted life to the test life is shorter at higher load factors within each spectrum (81-83, 84-86, 88-89, 90-92, 93-94). This is attributed to the changes in the constraint at the crack tip. All of the presented predictions assumed plane strain conditions in order to be slightly conservative overall. The higher the stresses the more likely plane stress occurs, especially during a high overload. This definite relationship between applied stress levels and prediction accuracy would suggest the need for a variable constraint factor which would be a function of the ratio for plastic zone diameter to the material thickness.

Table 2 also presents crack growth predictions using no interaction effects, i.e., linear cumulative damage. These predictions are surprisingly good. This indicates that the acceleration and retardation produced by the load interactions nearly negate each other for most of the spectra. Only specimens M-88 and M-89 had a sufficiently high overload such that retardation dominated the life. Specimens M-93 and M-94 were dominated by crack growth acceleration as is obvious from the very long life predicted with no load interaction.

CONCLUDING REMARKS

This paper presented a phenomenological load-interaction model developed to predict crack growth propagation under any arbitrary load sequence. The present model is referred to as the Multi-Parameter Yield Zone (MPYZ) Load Interaction Model. Crack growth retardation and acceleration are accounted for by decreasing or increasing, respectively, the effective stress ratio used in a modified Forman's crack growth equation.

The presented MPYZ load interaction model in conjunction with the CGR-LaRC computer routine did a good job of predicting spectrum fatigue crack growth in 2219-T851 aluminum. However, the predictions were not perfect as illustrated by M-88 and M-89 where too much crack growth retardation was predicted. It is difficult to truly assess the prediction accurately since the validity of individual tests may be suspect due to a lack of replicate tests. Furthermore, many of the spectra were not a true test of a load interaction model since linear cumulative damage models worked well.

The MPYZ model has undergone many refinements during the past 4 years since phenomena such as crack growth acceleration and underload effects have been recognized and investigated. This, indeed, increases the general applicability of this model over those models capable of accounting only for retardation effects.

REFERENCES

1. Wheeler, O. E., "Spectrum Loading and Crack Growth," J. of Basic Eng., ASME, Vol. 94, Ser. D, No. 1, March 1972, p. 181.
2. Willenborg, J. D., Engle, R. M., Jr., and Wood, H. A., "A Crack Growth Retardation Model Using Effective Stress Concept," AFFDL-TM-71-1-FBR, January 1971.
3. Elber, W., "The Significances of Fatigue Crack Closure," ASTM STP 486, 1961, pp. 230-242.
4. Gray, T. D. and Gallagher, J. P., "Predicting Fatigue Crack Retardation Following a Single Overload Using a Modified Wheeler Model," ASTM STP 590, 1975.
5. Gallagher, J. P. and Hughes, T. F., "Influence of Yield Strength on Overload Affected Fatigue Crack Growth Behavior in 4340 Steel," AFFDL-TR-74-27, July 1974.
6. Bell, P. D. and Creager, M., "Crack Growth Analysis for Arbitrary Spectrum Loading," AFFDL-TR-74-129, October 1974.
7. Gallagher, J. P., "A Generalized Development of the Yield Zone Models," AFFDL-TM-FBR-74-28, January 1974.
8. Hagemeyer, J. W., "Overload Induced Retardation of Fatigue Cracks in Several Aluminum and Titanium Alloys," General Dynamics ERR-FW-1779, Dec. 1976.
9. Johnson, W. S. and Hagemeyer, J. W., "Yield Stress Consideration for Selecting Materials Subjected to Spectrum Loads," International J. of Fracture, Vol. 13, No. 4, August 1977.

10. Hillberry, B. M., Alzos, W. X., and Skat, A. C., "The Fatigue Crack Propagation Delay Behavior in 2024-T3 Aluminum Alloy Due to Single Overload/Underload Sequences," Air Force Flight Dynamics Lab Report, AFFDL-TR-75-96, August 1975.

11. Himmelein, M. K. and Hillberry, B. M., "The Effect of Stress Ratio and Overload Ratio on Fatigue Crack Delay and Arrest Behavior Due to Single Peak Overloads," ASTM STP 590, 1975.

12. Probst, E. P. and Hillberry, B. M., "Fatigue Crack Delay and Arrest Due to Single Peak Tensile Overloads," AIAA Journal, 12:3, March 1974, pp. 330-335.

13. Trebules, V. W., Roberts, R., and Hertzberg, R. W., "Effects of Multiple Overloads on Fatigue Crack Propagation in 2024-T3 Aluminum Alloy," ASTM STP 536, 1973, pp. 115-146.

14. Hall, L. R., Shah, R. C., and Engstrom, W. L., "Fracture and Fatigue Crack Growth Behavior of Surface Flaws and Flaws Originating at Fastener Holes," AFFDL-TR-74-47, May 1974.

15. Johnson, W. S., "CGR, An Improved Computerized Model to Predict Fatigue Crack Growth Under Spectrum Loading," NSRDC Report 4577, Jan. 1975.

16. Johnson, W. S. and Spamer, T., "A Users Guide to CGR-GD, A Computerized Crack Growth Predicting Program," General Dynamics Report FZ5-241, Nov. 1976.

17. Chang, J. B. and Stolpestad, J. H., "Improved Methods for Predicting Spectrum Loading Effects - Phase I Report," Vol. II - Test Data, Air Force Flight Dynamics Lab Report, AFFDL-TR-79-3036, March 1978.

18. Mills, W. J., Hertzberg, R. W., and Roberts, R., "Load Interaction Effects on Fatigue Crack Growth in A514F Steel Alloy," Cyclic Stress-Strain and Plastic Deformation Aspects of Fatigue Crack Growth, ASTM STP 637, American Society of Testing and Materials, 1977, pp. 192-208.

19. Newman, J. C., Jr., "Prediction of Fatigue Crack Growth Under Spectrum Loading Using a Crack Closure Model," Methods and Models for Predicting Fatigue Crack Growth Under Random Loading, ASTM STP , 1981, pp.

20. Hudak, S. J., Jr., Saxena, A., Bucci, R. J., and Malcolm, R. C., "Development of Standard Methods of Testing and Analyzing Fatigue Crack Growth Rate Data," AFML-TR-78-40, May 1978.

21. Johnson, W. S., "Prediction of Constant Amplitude Fatigue Crack Propagation in Surface Flaws," ASTM STP 687, American Society for Testing and Materials, 1979, pp. 143-155.

22. Johnson, W. S., Rister, W. C., and Spamer, T., "Spectrum Crack Growth in Adhesively Bonded Structure," J. of Eng. Material and Tech., ASME Trans. Vol. 100, No. 1, Jan. 1978, pp. 57-63.

23. Tada, H., Paris, P. C., and Irwin, G. R., "The Stress Analysis of Cracks Handbook," Del Research Corp., 1973.

24. Forman, R. G., Kearney, V. E., and Engle, R. M., "Numerical Analysis of Crack Propagation in Cyclic-Loaded Structures," J. of Basic Eng., Trans. of ASME, Series D, Vol. 89, No. 3, Sept. 1967, pp. 459-464.

TABLE 1.- MATERIAL PROPERTIES FOR 2219-T851 USED FOR PREDICTION

CRACK GROWTH CONSTANTS	MPYZ MODEL PARAMETERS
$C = 4.626 \times 10^{-9}$	$A = 1.0$
$n = 3.171$	$B = 2.3$
$K_c = 88\ MN\text{-}m^{-3/2}$	$Y = 0.0$
$\Delta K_{TH} = 3.3\ MN/m^{-3/2}$	$Z = 0.5$
Yield stress = 345 MPa	
Ultimate stress = 448 MPa	

TABLE 2.- CRACK LIFE PREDICTION RESULTS

SPECTRUM TYPE	SCALE FACTOR	SPECIMEN	a_i	a_f	N_{TEST}	PREDICTIONS*	
						LOAD INTERACTION N_{PRED}/N_{TEST}	NO LOAD INTERACTION N_{PRED}/N_{TEST}
Air-to-Air Fighter	0.2	M-81	0.16	0.5125	115,700	1.08	1.27
	0.3	M-82	0.15	1.395	58,585	0.78	0.85
	0.4	M-83	0.15	0.9175	18,612	0.85	0.89
Air-to-Ground Fighter	0.2	M-84	0.1575	2.2	268,908	1.01	1.09
	0.3	M-85	0.144	1.735	95,642	0.78	0.81
	0.4	M-86	0.1525	1.29	36,397	0.71	0.70
Instrumentation Navigation Fighter	0.3	M-88	0.15	1.805	380,443	1.50	0.73
	0.4	M-89	0.15	1.5125	164,738	1.40	0.62
Composite Mission Fighter	0.2	M-90	0.1525	2.03	218,151	0.99	1.09
	0.3	M-91	0.15	1.4225	65,627	0.84	0.87
	0.4	M-92	0.15	1.1625	22,187	0.90	0.88
Composite Mission Transport	0.2	M-93	0.25	0.5375	1,354,024	0.94	3.00
	0.3	M-94	0.2575	0.375	279,000	0.86	1.81
					Mean	0.97	1.12
					Std Dev	0.24	0.64
					Std Error	0.18	0.38

*Plane strain conditions assumed.

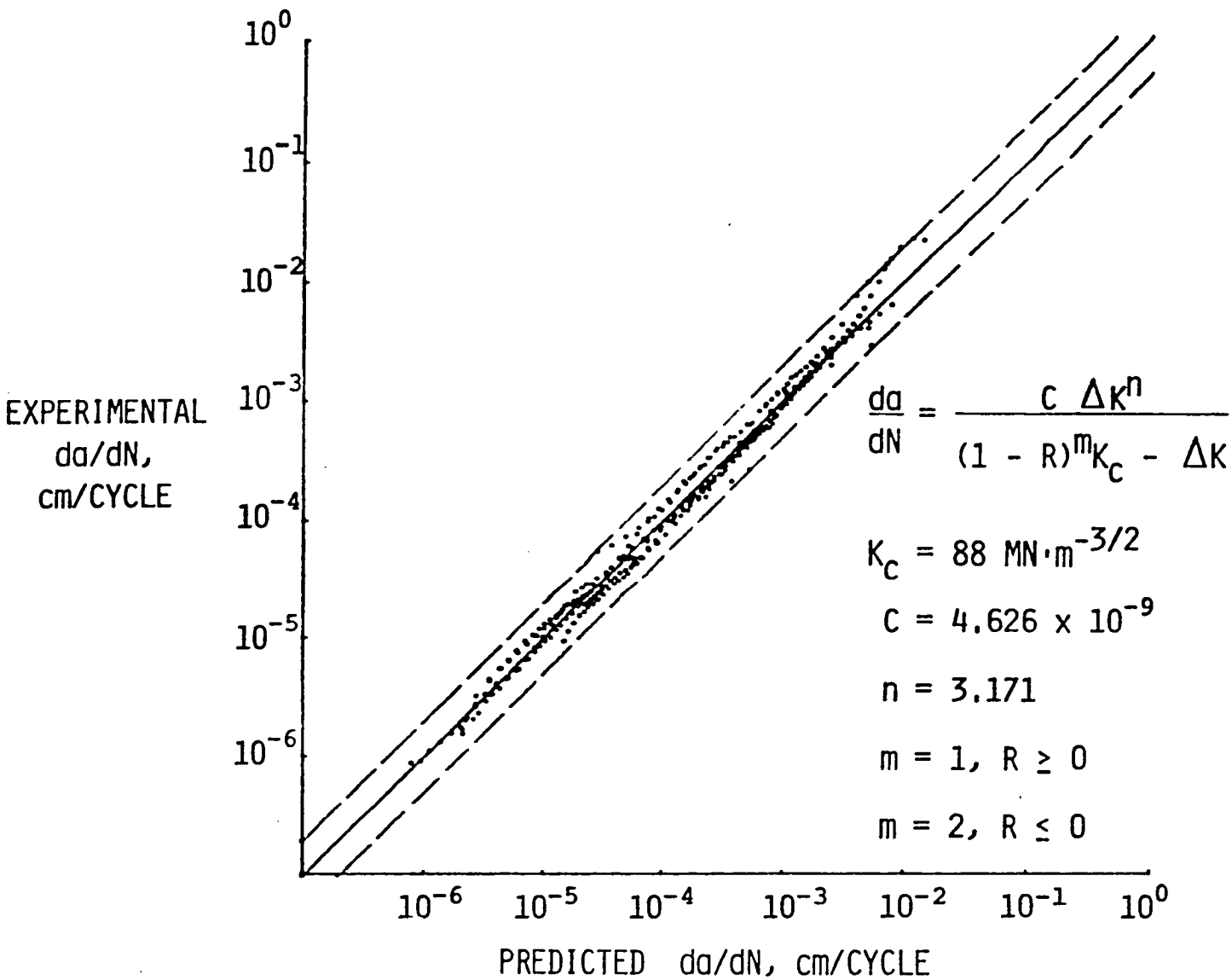

Figure 1.- Constant amplitude crack growth rate correlation.

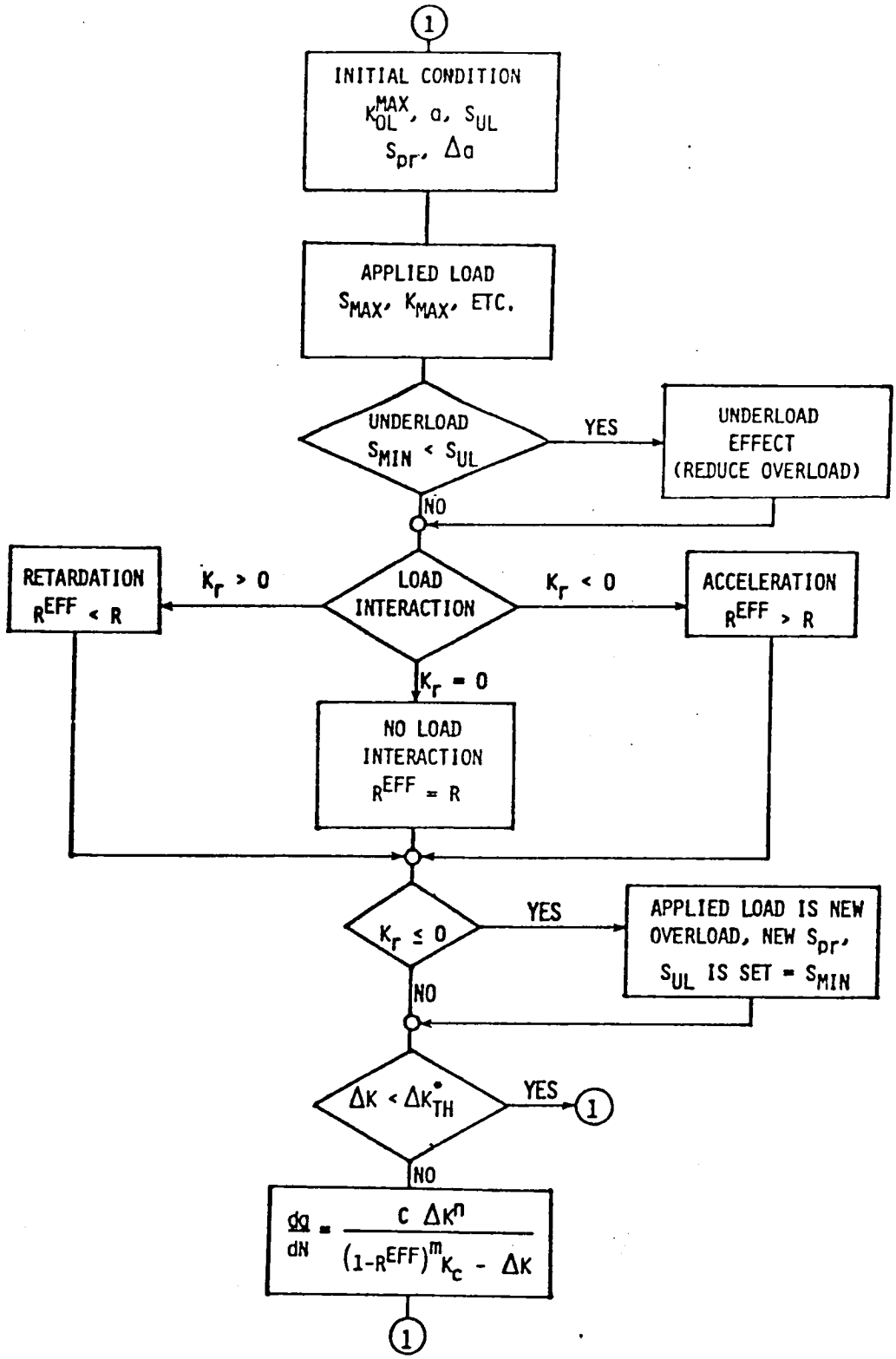

Figure 2.- Flow chart of the MPYZ load interaction model.

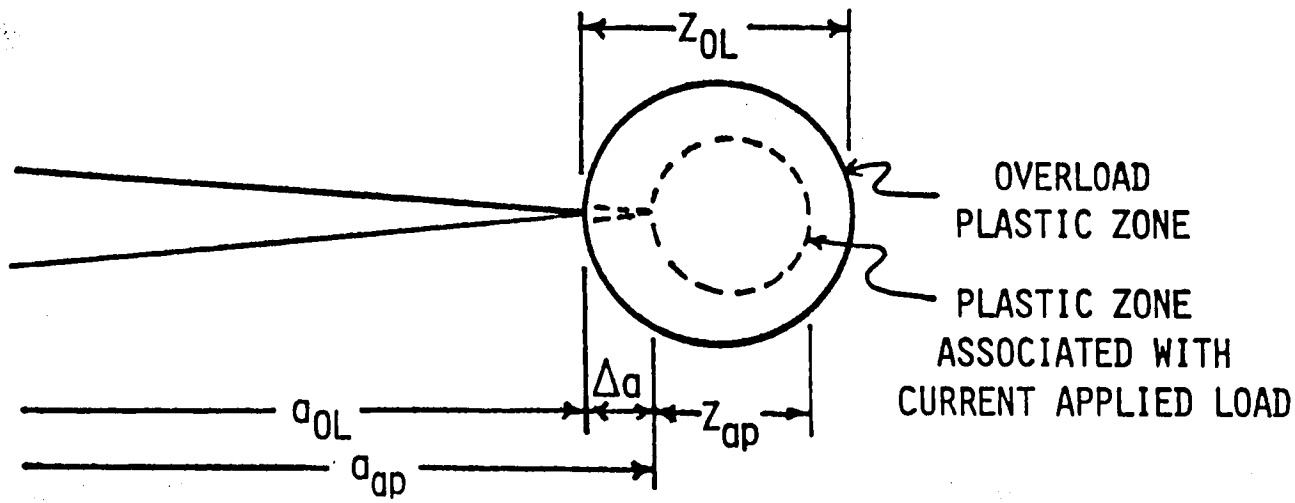

Figure 3.- Plastic zones at crack tip.

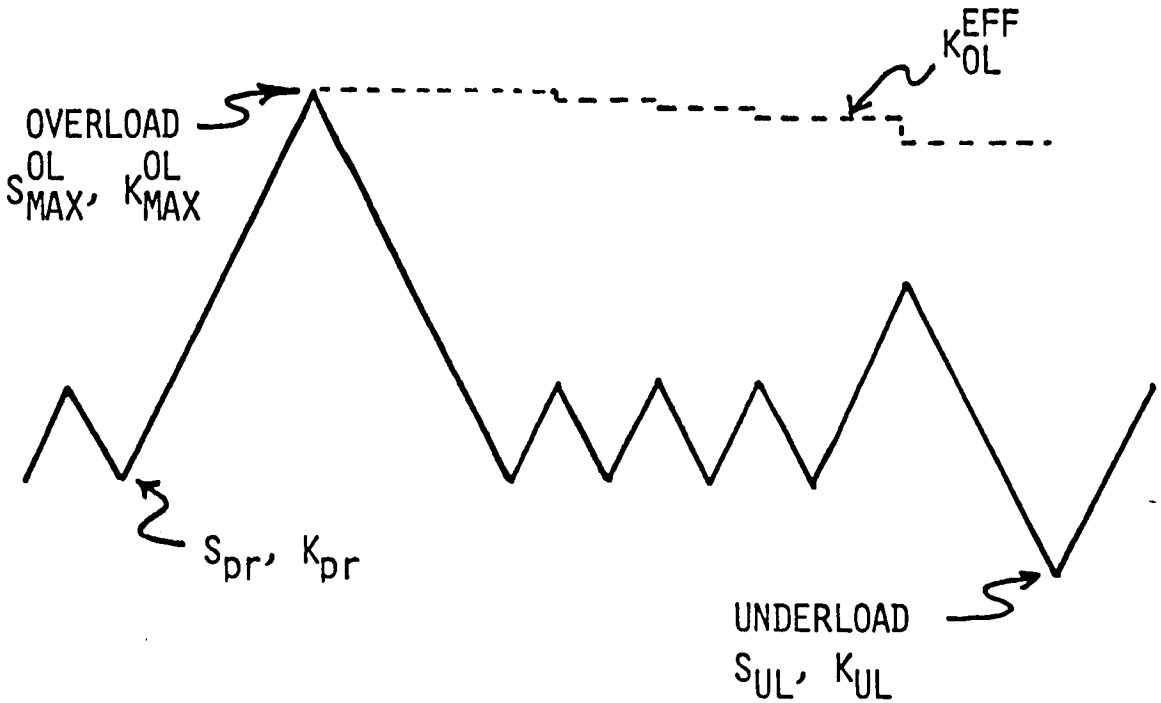

Figure 4.- Example spectrum sequence.

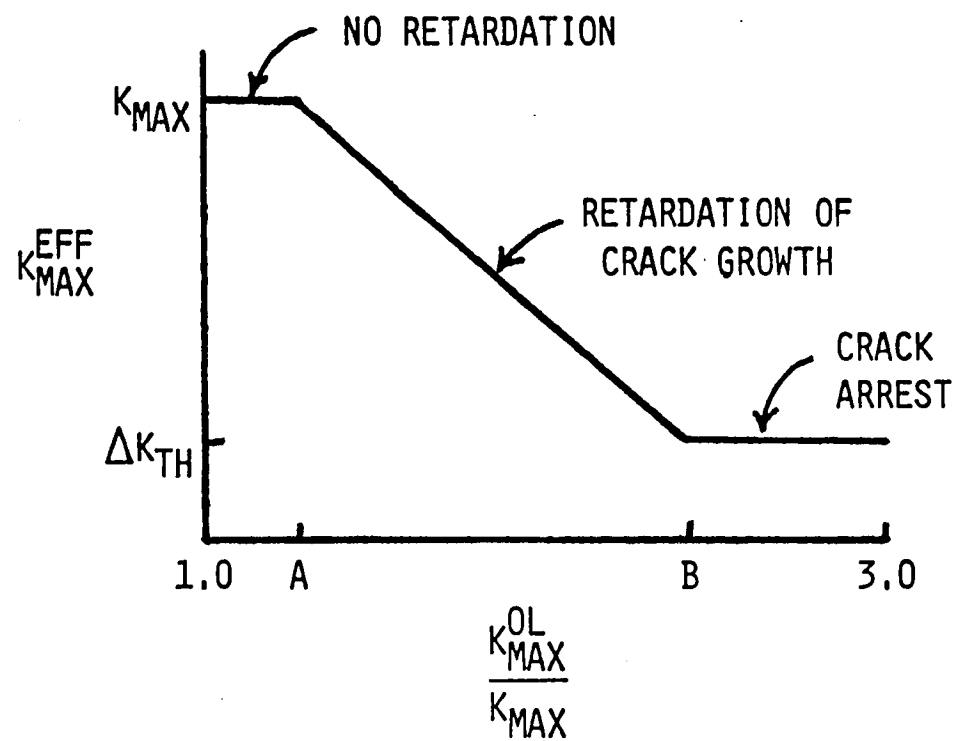

Figure 5.- Schematic of retardation in the MPYZ load interaction model.

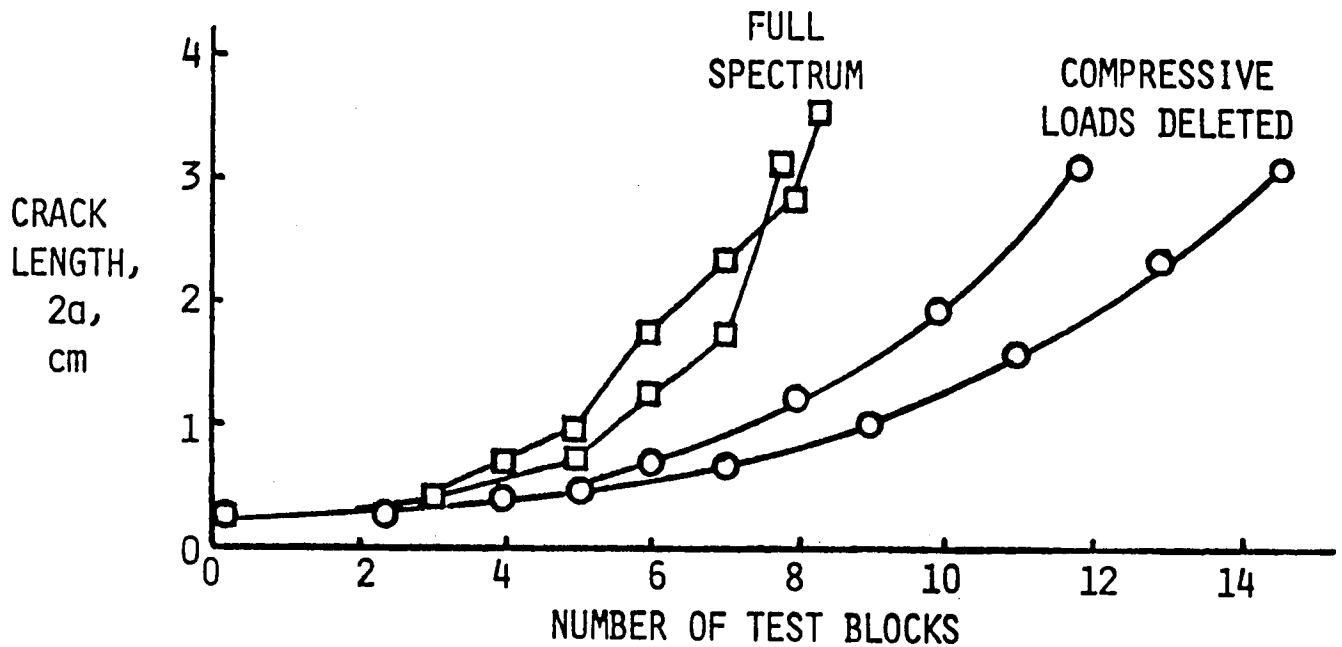

Figure 6.- The effect on crack growth of truncating negative loads from a flight-by-flight fighter spectrum.

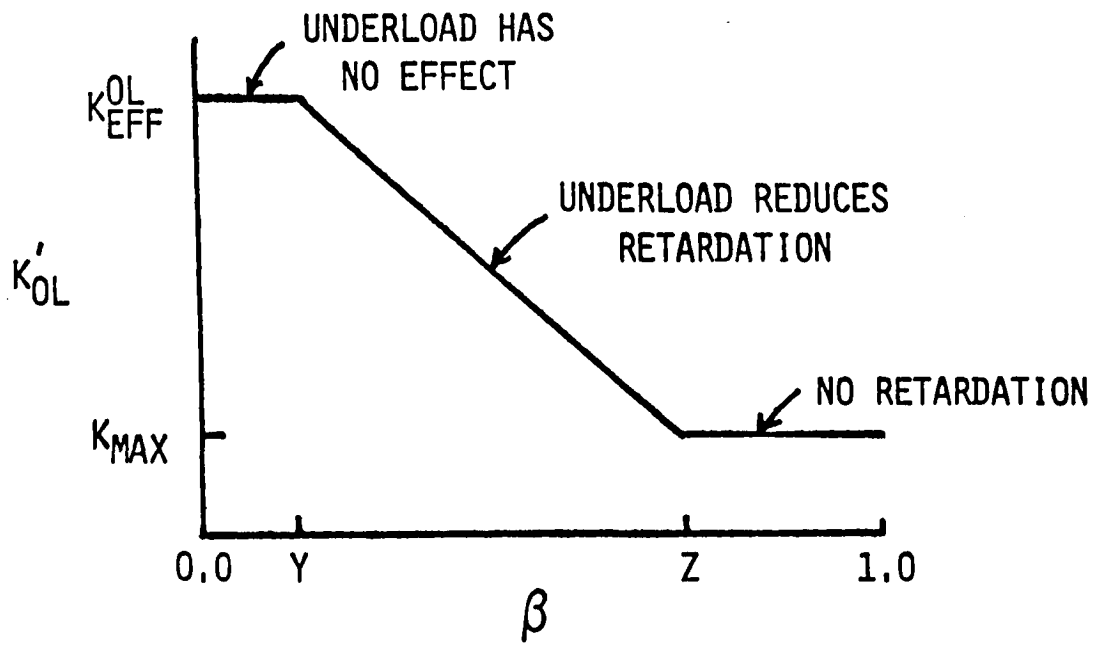

Figure 7.- Schematic of underload effects in the MPYZ load interaction model.

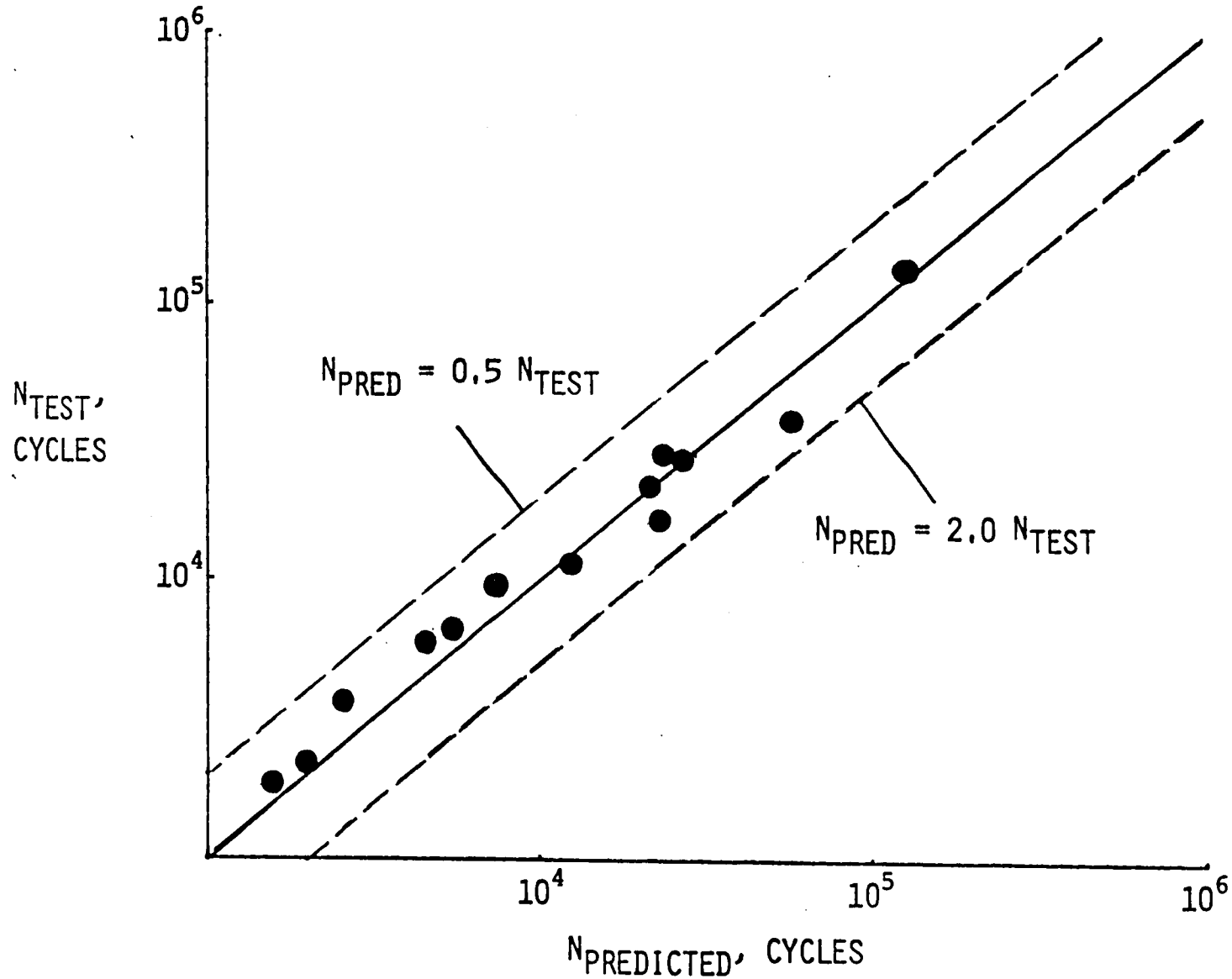

Figure 8.- Correlation of predicted life, N_{PRED}, to test life, N_{TEST}.

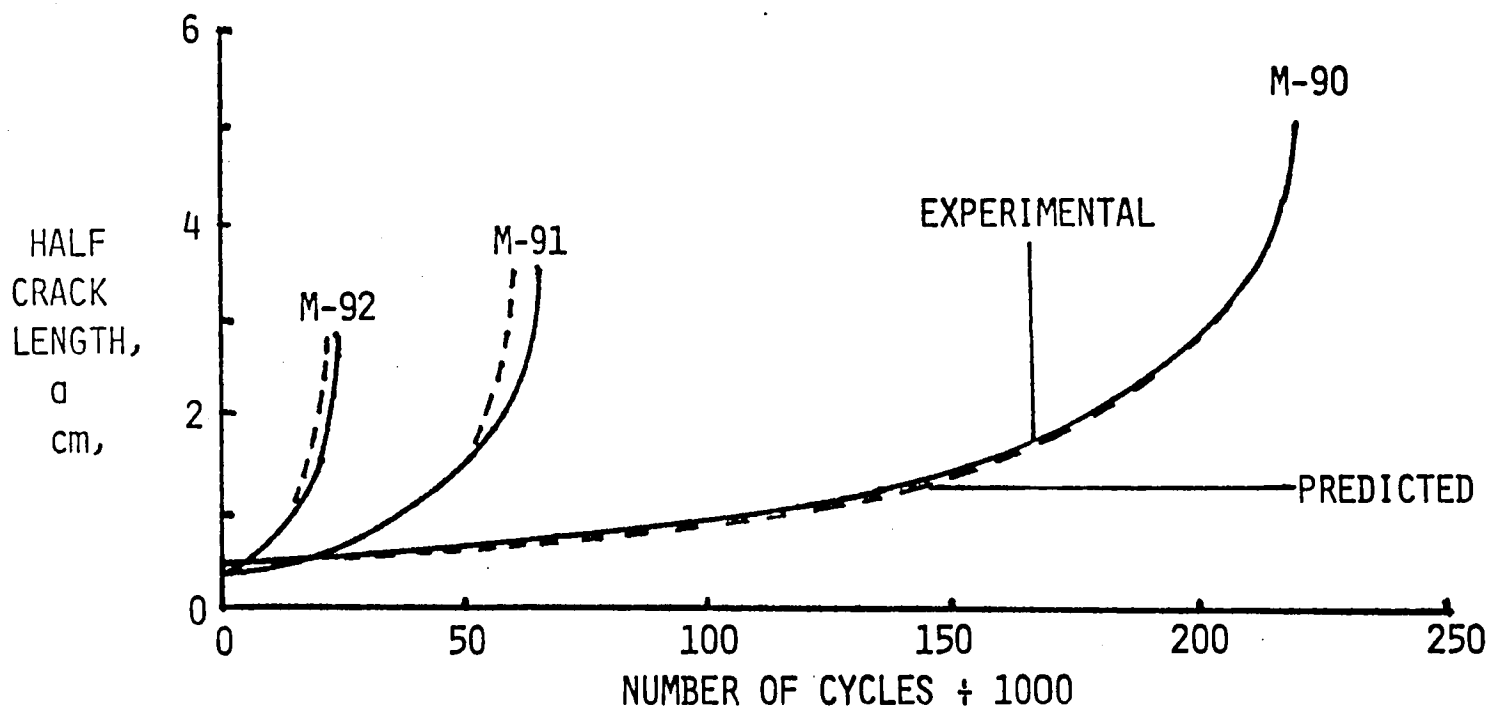

Figure 9.- Example crack growth predictions for the fighter composite mission spectra.

1. Report No.	2. Government Accession No.	3. Recipient's Catalog No.
NASA TM-81890		

4. Title and Subtitle	5. Report Date
MULTI-PARAMETER YIELD ZONE MODEL FOR PREDICTING SPECTRUM CRACK GROWTH	September 1980
	6. Performing Organization Code
7. Author(s)	8. Performing Organization Report No.
W. S. Johnson	
9. Performing Organization Name and Address	10. Work Unit No.
NASA Langley Research Center Hampton, VA 23665	506-53-53-01
	11. Contract or Grant No.
	13. Type of Report and Period Covered
12. Sponsoring Agency Name and Address	Technical Memorandum
National Aeronautics and Space Administration Washington, DC 20546	14. Sponsoring Agency Code

15. Supplementary Notes

This paper was submitted to the American Society for Testing and Materials for inclusion in a Special Technical Publication entitled "Methods and Models for Predicting Fatigue Crack Growth Under Random Loading."

16. Abstract

A systematic technique is presented for modeling crack growth load interaction effects due to spectrum loading. The Multi-Parameter Yield Zone (MPYZ) model accounts for crack growth retardation, acceleration, and underload effects. The load interactions are attributed to the residual stress intensity due to the plastic deformation at the crack tip. As part of an ASTM E24.06.01 round-robin effort, fatigue crack growth was predicted and compared with test data for a variety of spectrum loadings.

17. Key Words (Suggested by Author(s))	18. Distribution Statement
Spectrum loads Fatigue crack growth 2219-T851 aluminum Crack growth retardation Crack growth accelerations Load interaction Underload effects	Unclassified - Unlimited Subject Category 39

19. Security Classif. (of this report)	20. Security Classif. (of this page)	21. No. of Pages	22. Price*
Unclassified	Unclassified	34	A03

* For sale by the National Technical Information Service, Springfield, Virginia 22161